

Chapter 2

Western Disturbances – Dynamics and Thermodynamics

Abstract To further expand our knowledge of the weather systems called western disturbances (WDs), in this chapter we present the dynamical basis of WDs. The mechanism of WD formation with details on the evolution of such storms are discussed, and a detailed explanation of the energetics and thermodynamics of the winter storms provided. The various studies on WDs using various tools such as satellite information or numerical modelling techniques are reviewed and summarized. Last but not the least, the influence of surface variability in terms of orography and land use – land cover impacts on WDs are in this chapter.

The previous chapter dealt with WDs in an introduction that detailed providing the typical structure and origin of these extra-tropical systems. To further expand our knowledge of these systems, this chapter develops the dynamical understanding of the WDs. The various studies on WDs using various tools such as satellite information or numerical modelling techniques are have been reviewed and summarized. And finally the influence of surface variability in terms of orography and changes in land use and land cover changes on WDs are discussed in this chapter.

Before proceeding with the working sections of the chapter detailing information about the WDs we briefly review the Himalayas. As will be discussed later, the Himalayas have a major impact on WDs and in further chapters we will note that there is a reciprocal impact from WDs on the Himalayas also. Hence, an introduction to the Himalayan mountain range is prudent. The Himalayas have been illustrated clearly in the Fig. 1.1 in the previous chapter. A detailed idea of the Himalayan extent and topography has been illustrated in Fig. 2.1. The Himalayas extend 2500 km which stretches from 34 to 36°N, 27° E and 27–28°N, 90° E with a width of 250–400 km (Barry 2008). West to east this mountain range is divided into regions called as the north-western Himalayas, central Himalayas and eastern Himalayas. Bordering on the northern edge of the Himalayas is the Tibetan Plateau. Moreover, the western part of the Himalayas is bordered by the Hindu-Kush range. According to Barry (2008), the Himalayas from north to south can be divided into three major ranges. The Greater Himalayas in the north have the highest mountains, with an average height of 6000 m. South of this range, in the middle, is the Lesser Himalayas with average peak height of 2000–3300 m. And down south the range is called the outer Himalayas or the Siwaliks which are shorter with peak height

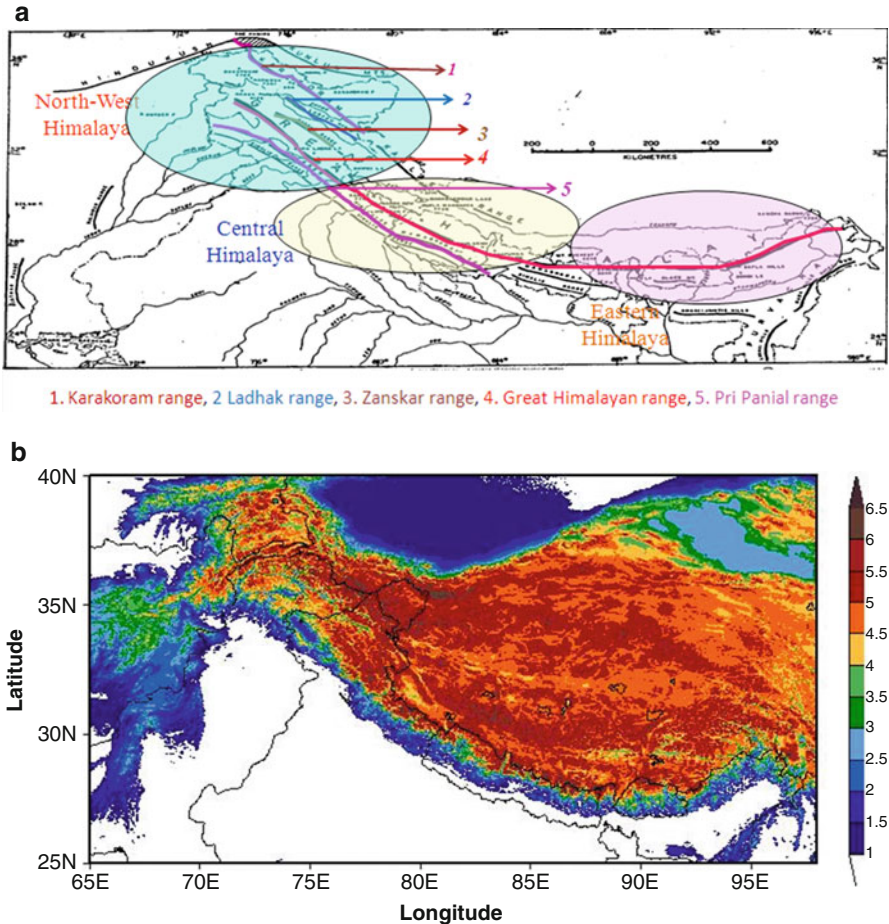


Fig. 2.1 (a) Schematic representation of cascading Himalayan mountain ranges (Pir Panjal- Great Himalaya-Zaskar-Ladhak-Karakoram) and western-central-eastern Himalayan region (b) Topographic ($\times 10^3$ m) overview of the Himalayas

averaging 900–1200 m. The Himalayas have a natural variability in land-cover patterns. Thus, the land-use and land-cover variability and topographic heterogeneity are the characteristic features of the Himalayas (Dimri 2012). The climatic conditions for the temperature parameter show variability over the Himalayan region due to the variation in the orography (Dimri 2004) and the land use (Dimri 2009), as also reported in the study Dash et al. (2007). Temperature predictably decreases with altitude, and the mountain range also shows a normal latitudinal gradient over the lower Himalayas. Precipitation patterns over the Himalayas also have a large variation due to the heterogeneous topography and variation in the surface cover (Dimri 2012). From an ecological stand point, the Himalayas have an outer monsoon forest, a zone of inner coniferous forest, and a border zone in the north of arid steppe.

With increased human intervention, there has been clear changes in the land-use and land-cover variability of the region especially because of more unplanned urbanization, agriculture and industrialization (Kala 2014).

The Himalayas, due to their unique geographical position, provide a physical barrier that plays an important role in global weather patterns (Fig. 2.1), acting as a heat source during the summer and a heat sink during the winter. Topographic heterogeneity, land-use variability, and varying snow-cover extent are important climate actors affecting the Indian summer monsoon (ISM) (Boos and Kuang 2010). During winter, the Himalayan region is prone to severe weather and the large amounts of snowfall produced by WDs (Schiemann et al. 2009). Regional spring snowmelt runoff contributes 15–44 % of the discharge to the tributaries of the Indus, and 6–20 % of the Ganges discharge (Ramasastry 1999). Spring runoff becomes especially important in the case of a delayed monsoon onset (Bamzai and Shukla 1999; Liu and Yanai 2002), and is a factor in pre-monsoon flooding and landslides (Agrawal 1999; Thayyen et al. 2012).

2.1 Dynamics of Western Disturbances

In this section we examine the dynamics, energetics and thermodynamics of WDs. WDs are synoptic systems with associated large-scale circulation patterns. Various process studies into the energy and water budgets for large-scale synoptic systems are required to determine the dynamics of the systems. After reviewing many papers, Gupta and Mandal (1987) as well as Raju et al. (2011) noted the importance of large-scale synoptic systems in the generation, transfer and transformation of kinetic energy in the middle latitudes and their various patterns in the lower latitudes. The available potential energy for the extra-tropical cyclonic weather systems is drawn from the latitudinal/meridional temperature gradient (between different latitudes) (Dimri et al. 2004). The difference in the temperatures between the tropics and mid-latitudes or even the polar region play a significant role in generating the extra-tropical cyclones. The literature review also suggested that the WD kinetic-energy budget will be a more interesting topic to study since WDs are systems that move in the borderline zone of tropics and extra-tropics (Raju et al. 2011). Although WDs are considered similar to extra-tropical systems, they differ from such systems because their frontal structures dissipate due to the friction of the surface as they migrate long distances. Also, their movement across Himalayan orography causes energy changes that are different than those seen in the usual mid-latitude systems. A synthesis of the various studies on WD kinetic-energy budget is provided here for a deeper understanding of the WDs.

A study by Ananthkrishnan and Keshavmurthy (1973) analysed the generation of kinetic energy over India during the winter season by diagnosing the meridional wind and the zonal wind flow. The study reported that the adiabatic kinetic energy within WDs is consumed by zonal wind flow along its track due to enhanced meridional wind flow and vice versa. Gupta and Mandal (1987) explained the behavior of

the kinetic-energy generation function during a WD. Their study revealed that the increase (decrease) in the kinetic energy content of the system could not be related directly to the positive (negative) contribution of the kinetic-energy generation function. Further, the zonal component of the kinetic energy generation function acted as a source, while the meridional component behaved as a strong sink in the upper levels throughout the life cycle of the system. Analysis of meteorological global reanalysis datasets enables researchers to examine the unique characteristics of specific synoptic events. Many of these reanalyses depict the large-scale circulation characteristics of WDs reasonably well despite weak constraints due to data paucity in the Himalayas (Mohanty et al. 1998, 1999). As an example, Roy and Bhowmik (2005) successfully used gridded datasets of the Indian Meteorological Department global- model output to thermodynamically analyse the WDs over the Delhi region. The study revealed that there is external advection of water vapor over a region as a consequence of the passage of WDs. The atmosphere during the winter season over the region is relatively dry and cannot result in precipitation due to convection at the local level. Hence, the external source of moisture incursion is a necessity for the WD related winter precipitation. In association with the moisture influx, convective activity is observed as the energy realized when the conditional instability is released, the latter termed the convective available potential energy (CAPE). The CAPE values increase during a WD passage, providing the required energy for the storm to form. According to Agnihotri and Singh (1987), during winters the shortwave solar radiation is absorbed mostly in the lower levels of the atmosphere due to the presence of the moisture. During WD occurrences due to low level moisture incursion, there is enhanced absorption of the incident solar radiation in the lower levels, which is another source of energy for the storm. Mohanty et al. (1999) performed a comparative analysis of the dynamical and thermodynamical characteristics between weak and active WD using observational analysis. The study reports higher amounts of precipitable water and higher convergence of horizontal heat flux during an active WD than in a weak WD. The role of the Himalayan orography in blocking and guiding the integrated moisture fluxes within the model reanalysis for an active WD over northern India is shown by Raju et al. (2011), confirming the early diagnosis of Ananthakrishnan and Keshavmurthy (1973). It reported that zonal and meridional formation of kinetic energy was in opposition to generation. The study also showed a strong rise in the convergence of the flux of kinetic energy and weak adiabatic production of kinetic energy during the passage of an intense WD. Towards the centre of the low pressure area of the WD, destruction of kinetic energy took place, whereas generation of the energy occurred west of the centre of an intense WD.

Access to satellite imagery changed tools and methodologies in weather forecasting and have proven to be essential elements of improved effectiveness (Houghton 1987). Studies related to the WDs using satellite data have provided detailed information on the topic. The first synoptic charts for India, with input from satellite imagery showing jets and cloud systems, were produced in 1970 (Srinivasan 1971). This study reported the formation of the clouds associated with troughs in the SWJ which is indicative of the precipitation associated with the WDs. Satellite

imagery and charts available were used to analyse the cloud bands associated with WDs, classifying cloud patterns in terms of the relationship between geometry and cloud area (Rao and Moray 1971). Such structure-based cloud imagery helped in assessing the evolution of WDs over time and provided an analysis of the life cycle of an evolving WD. Based on 10 years of satellite information, three broad categories were suggested by Agnihotri and Singh (1982). A significant finding of this study was that there are important secondary extra-tropical depressions traveling with large-scale westerlies and approaching northwest India. Detailed analysis of the cloud formation associated with the WDs are described in the previous chapter.

Other than using satellite imagery to study cloud systems associated with the WDs, this imagery has been used to analyse other details about these systems. Using NOAA-6 satellite products, Sharma and Subramaniam (1983) pointed out the linkages of WDs with the low-level easterly troughs responsible for intensification of the WD. They provided further support that this linkage caused expanded associated precipitation far to the south. A relationship between cloud-top temperatures and WD rainfall in the relatively drier month of November was proposed by Veeraraghavan and Nath (1989). They used Arkin's methodology to estimate the precipitation caused by WDs using the cloud-top temperatures. But this methodology did not provide accurate rainfall estimates when compared with the actual average rainfall based on the data provided by the gauge stations because the methodology was not used on a region of variable orography like Himalayas. Puranik and Karekar (2009) used satellite observations from multiple platforms to delineate the cold-air intrusion and the moisture pathways. Their objective was to demonstrate the capability of Advanced Microwave Sounding Unit -B (AMSU-B), flying onboard the NOAA satellite, to monitor WDs in five different microwave frequencies. Now data assimilation of satellite data into modelling techniques are providing yet greater accuracy for the model simulated outputs when compared with the observational analysis. Rakesh et al. (2009) is one of the studies including satellite data into numerical weather prediction.

Satellite information has been an important tool in studying the interaction of the mid-latitude systems with tropical systems. An important aspect of the interaction between the tropics and mid-latitudes is the emergence of cloud surges, which are due to the interaction of tropical and mid-latitude flows, and are clearly visible in satellite imagery. When the existence of large amplitude troughs in subtropical westerlies impinge on low-latitude synoptic disturbances, this first 'interaction' shows signs of cloud deformation north-eastward from the lower latitudes Kalsi and Halder 1992). Such interactions during summer monsoon months add to increased monsoonal flow. A similar case of tropical and extra-tropical interaction led to the massive disaster over the Kedarnath region in June 2013. Interaction between WD and MT caused the formation of dense clouding and resulting in the heavy precipitation observed over northern India (IMD 2013), as also seen by satellite imagery. This cloud system was termed a transient cloud system (Pandey and Pandey 2014; Chevuturi and Dimri in review). Detailed analysis of interaction of tropical and mid-latitude systems are described in the next chapter.

2.2 Modelling Studies Related to Western Disturbances

A survey of modelling attempts of WD events is described here. Table 2.1 presents the framework associated with various modelling studies and major findings of the studies. The main focus is on significant milestones in WDs' modelling studies that enhanced process understanding and model improvement. While greater understanding of the WDs needs no justification, model improvement is important for the improvement in forecasting and prediction of the WDs. The first mathematical description of cyclonic waves in the baroclinic westerlies was introduced by Charney (1947), which provided a theoretical basis for numerical weather prediction (Charney 1948; Charney et al. 1950). Here, we mainly rely on existing dynamical numerical models of WDs. Rao and Rao (1971) considered that the observed zonal wind profile is unstable with respect to the small superimposed disturbance, most notably for a perturbation wavelength of around 7000 km at 28°N. Such baroclinic instability is a possible mechanism for energy release and the development of a WD. They also analysed the periodicity and wavelength of the WD in the form of wave disturbances. They found out that WDs have a periodicity of about 9 days and a wavelength of about 6.0×10^6 m in early stages and 8.5×10^6 m in the later stages of development. Ramanathan and Saha (1972) applied a primitive equation in a barotropic model at 500 hPa to predict the evolution of WDs and investigated the role of initial and boundary conditions on forecast accuracy. The study used two cases of WDs to analyse the forecast ability of the model using east-west cyclic boundary conditions. They developed encouraging and important applications of dynamical models to predict WD movement. Chitlangia (1976) employed a moving coordinate system to study the mean structure of a WD. The study used data from six WD cases in the model. Hoskins and Karoly (1982), using a steady-state-linearized- five-layer baroclinic model, established the role of subtropical forcing to produce appreciable response in mid- and high latitudes. In low latitudes, it establishes that longer wavelengths propagate poleward and eastward, whereas shorter wavelengths are trapped in the equatorward side of the jet. This trapped jet enhances the evolution of embedded WDs. A comprehensive analysis of a WD simulated within a global spectral model reported by Dash and Chakrapani (1989) showed improvement in forecast skill with respect to geopotential heights and wind magnitude associated with a WD, and thus associated precipitation. deSilva and Lindzen (1993) investigated stationary waves in the northern hemisphere winter using stationary and time-dependent, linear primitive equation models. In tandem with Nigam and Lindzen (1989), they found that small displacements of the SWJ causes significant changes in stationary wave response right in the troposphere and in the lower troposphere. This behavior could be used for long-range forecasting of the associated synoptic weathers such as WDs. Predictability of precipitation associated with WDs increased with the introduction of boundary-layer and convection schemes in numerical models (Azadi et al. 2001; Das et al. 2003; Das 2005; Hatwar et al. 2005; Dimri and Chevuturi 2014; Chevuturi et al. 2014).

Table 2.1 Summary of the WD studies using modelling efforts

| Reference | WD case discussed | Model used | Horizontal model Resolution | Parameterization Schemes | | Significant findings |
|----------------------------|--|---|-----------------------------|--|---------------------|---|
| | | | | Convective | PBLs0073 | |
| Rao and Rao (1971) | 11–17 Dec 1963 | Observational data used | | | | The WD development shows similar characteristics to a baroclinically unstable disturbance. |
| Ramanathan and Saha (1972) | 22–25 Dec 1968; 11–14 Jan 1969 | Primitive equation limited-area barotropic model | 2.5° | | | Forecast of WD with the limited area model could generally predict the movement of WD, but required to improve resolution and reduce forecast error. |
| Chitlangia (1976) | 4–5 Jan 1959; 3–4 Feb 1959; 20–21 Jan 1962; 25–26 Jan 1962; 23–24 Feb 1962; 19–20 Jan 1965 | Moving coordinate system (empirical model) | 1° | | | During a WD, the vertical structure of atmosphere shows more complex characteristics than an extra-tropical depression with a simple two layer model. |
| Dash and Chakrapani (1989) | 27 Feb–3 Mar 1982 | Global spectral model (IIT Delhi) | | | | The forecast fields of 24 h accumulated precipitation and wind circulation patterns show agreement with the respective analysis. |
| Gupta et al. (1999) | 27–30 Dec 1994; 8–10 Jan 1995; 15–17 Jan 1996; 19–21 Jan 1997 | NCEP T80, 18 layer global spectral model (NCMRWF) | 160 km | | | The model is able to forecast intensity and extent of winter systems 72h in advance but not able to provide point specific predictions. |
| Azadi et al. (2001) | 18–21 Jan 1997 | MM5 (V2.12) | 60 km | Kuo, Grell, Kain-Fritsch, Betts-Miller | Blackadar, Hong-Pan | Hong-Pan PBL scheme and Betts-Miller cumulus scheme give better results as compared to the other parameterization schemes. |

(continued)

Table 2.1 (continued)

| Reference | WD case discussed | Model used | Horizontal model resolution | Parameterization Schemes | | Significant findings |
|----------------------|----------------------------------|---|-----------------------------|---|---------------------|---|
| | | | | Convective | PBLs/0073 | |
| Das (2002) | 14–16 Sep 2001 | MM5 | 90 km, 30 km, 10 km | Grell | Hong-Pan | Results show that model forecasts of WD and associated wind and precipitation compare well with the observation over the region. |
| Das et al. (2003) | 14–16 Sep 2001 | MM5 | 90 km, 30 km, 10 km | Grell | Hong-Pan | Model forecasts WD features are well depicted 72h in advance of the system. |
| Dimri (2004) | 21–25 Jan 1999 | MM5 (V2.12) | 90 km, 60 km, 30 km | Betts-Miller | Hong-Pan | Better representation of topographical features in the finer domain lead to improved simulation of WD and associated precipitation. |
| Dimri et al. (2004) | 21–25 Jan 1999 | MM5 (V2.12) | 60 km | Betts-Miller | Hong-Pan | Model simulation captured the movement and intensity of WD along with representing some fine structure not observed in the verification analysis. |
| Dimri et al. (2006) | 18–21 Jan 1997; 20–25 Jan 1999 | MM5 (V2.12) | 90 km, 60 km, 30 km | Kuo, Grell, Kain-Fritsch, Betts-Miller | Blackadar, Hong-Pan | Sensitivity analysis suggests that simulation of WD is better represented with combination of Hong-Pan PBL scheme and Betts-Miller convective scheme and finer horizontal model resolution. |
| Hatwar et al. (2005) | 13–17 January 2002; 5–8 Feb 2002 | IMD limited area analysis forecast system | 1° | Model description in detail in Krishnamurti et al. (1990) | | Precipitation patterns in the forecast compare well with the verification analysis but intensity of rainfall is under-predicted in the model output. |

| | | | | | | |
|--------------------------|---|--|---------------------|--------------|----------|--|
| Azadi et al. (2005) | 24 Mar 1993; 14 Feb 1995; 15 Jan 1996; 12 Mar 1998 | MM5 (V2.12) | 90 km, 60 km, 30 km | Betts-Miller | Hong-Pan | Model simulated synoptic system and associated features compares well with the analysis but shows slight bias which slows the system. |
| Das (2005) | 14–16 January 2002 | MM5 | 90 km, 30 km, 10 km | Grell | Hong-Pan | Forecasts upto 72 h show good capability of the model to predict rainfall over the mountainous regions. |
| Srinivasan et al. (2005) | 13–15 Mar 2001; 13–17 Jan 2002; 16–20 Feb 2003 | MM5 model (integrated with Snow cover model and statistical model) | 30 km | | | Improved avalanche prediction was observed on application of model predicted meteorological parameters. |
| Semwal and Giri (2007) | 30 Dec 2004–04 Jan 2005; 3–7 Feb 2007 | ARPS (V5.1.5) | 30 km | Kain-Fritsch | | Model simulates spatial distribution of the precipitation well and shows heterogeneous precipitation distribution on comparison with observation analysis in cases of merging WDs. |
| Dimri and Mohanty (2009) | 17–20 Jan 1997; 1–4 Feb 1997; 8–11 Feb 1997; 23–26 Feb 1997 | MM5 (V2.12) | 60 km | Betts-Miller | Hong-Pan | Simulation of active WDs with the model represent the associated mesoscale features well. |
| Hara et al. (2004) | 27–31 Dec 1990 | RAMS | 100 km | | | A simulation of quasi-stationary cyclone over southern slope of Himalayas is depicted as a topographic Rossby wave. |
| Semwal and Dimri (2012) | 1–4 Jan 2006; 31 Dec 2004–03 Jan 2005; 306 Feb 2005 | ARPS (V5.1.5) | 30 km, 10 km | Kain-Fritsch | | Complex topography and local meteorological effects impact the prediction of heterogeneous precipitation distribution. |

(continued)

Table 2.1 (continued)

| Reference | WD case discussed | Model used | Horizontal model Resolution | Parameterization Schemes | | Significant findings |
|----------------------------|--|--|-----------------------------|--|--------------------------|--|
| | | | | Convective | PBLs0073 | |
| Rakesh et al (2009) | 8–11 Feb 2007 | MM5 using 3DVar assimilation (with MODIS derived data) | | | | Forecast initialization with 3DVar approach shows improved results over simulation without incorporation of MODIS satellite datasets. |
| Dasgupta et al. (2012) | 23 Apr 2004 | MM5 (V3.4) using 3DVar assimilation | 90 km, 30 km, 10 km | Grell | Non local closure scheme | Improvement of precipitation forecasts is observed in simulation with 3D Var assimilation. |
| Dimri and Niyogi (2012) | 1980–2001 | RegCM3 | 60 km, 10 km | Grell | Hollslag | Model dynamical downscaling captures the topography and precipitation interaction well with finer resolution showing better results over WH. |
| Dimri et al. (2013) | 1990–2007 | HadRM3 and REMO | 0.23° (~2.5 km) | Mass flux (Gregory and Rowntree 1990) Mass flux (Tiedtke 1989) respectively | | Regional climate models captured features of dynamic and orographic forcing along with the associated precipitation mechanisms of WDs. |
| Thomas et al. (2013) | 17–18 Feb 2003; 21–22 Jan 2003; 10–11 Feb 2007; 27–28 Feb 2007; 11–12 Mar 2007 | WRF (ARW) | 45 km, 15 km | Grell Devenyi ensemble | Yonsei University (YSU) | For WDs simulations with ARW, RUC land surface parameterization is best suited. |
| Dimri and Chevuturi (2014) | 13–17 January 2002; 5–8 Feb 2002; 11–13 Feb 2002 | WRF (ARW) | 81 km, 27 km, 9 km | Kain-Fritsch | Yonsei University (YSU) | Eta grid-scale cloud and precipitation microphysics scheme; Yonsei University scheme and Kain-Fritsch scheme is found to be the best suite for WD studies over the Himalayan region. |

Benchmark studies for understanding the model of the physics and dynamics associated with WDs are reviewed next. From Azadi et al. (2001), Fig. 2.2a depicts the sea-level pressure chart during the 18–19 January 1997 WD event as seen in the observations reanalysis. In this figure, a clear surface low associated with the WD is observed. The corresponding MM5V3 (Mesoscale Model 5 Version 3) simulations for eight experiments with different combinations of planetary boundary layers and cumulus parameterization schemes are shown in Fig. 2.2b corresponding to the observation, Fig. 2.2a. This study provides guidance about the best combination of parameterization of physical processes from the various available options to configure the model to capture the dynamical structures of WDs. In this study, the analysis and prediction of field variables like sea level pressure, geopotential height, temperature, wind and precipitation are used as indicators of the best modelling output. Further, Dimri (2004), investigated the impact of topography and model resolution on the simulation of the WD on 23 January 1999 using MM5V3 and showed clearly that the evolution of the of WD in terms of its low pressure at 500 hPa is stronger when realistic topography is present (Fig. 2.3d, e, and f) than in a corresponding no topography experiment (Fig. 2.3a, b, and c). Similarly, more organized precipitation fields along the upwind slopes of the Himalayan complex are seen when realistic topography is present (Fig. 2.4d, e, and f) than in the corresponding no topography experiment (Fig. 2.4a, b, and c). Further, Dimri et al. (2004) study analysed the simulation of an intense WD using a mesoscale model (MM5) run at high resolution. According to the study, the model simulation at high resolution could capture the intensity and movement of the WD with accuracy. But the study of Azadi et al. (2005)

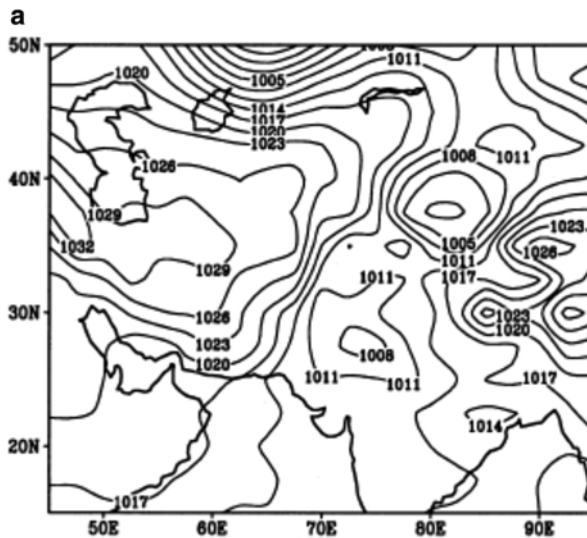


Fig. 2.2 Reanalysis of sea level pressure at 0000 UTC on (a) 19 Jan 1997 and (b) corresponding 24 h forecast of sea level pressure in 08 difference model experiments (Source: Met Appli. Azadi et al. 2001). Figure 1.3b is given on the next page

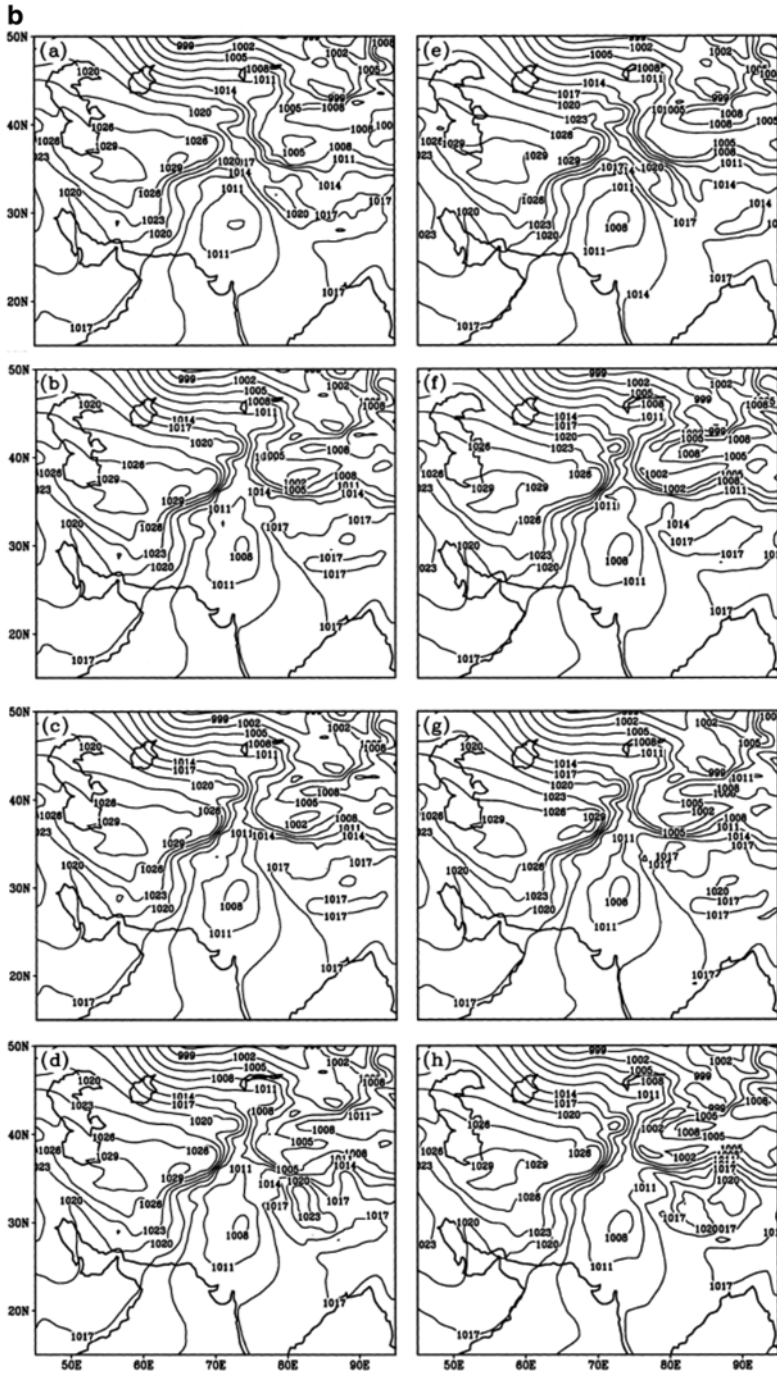


Fig. 2.2 (continued)

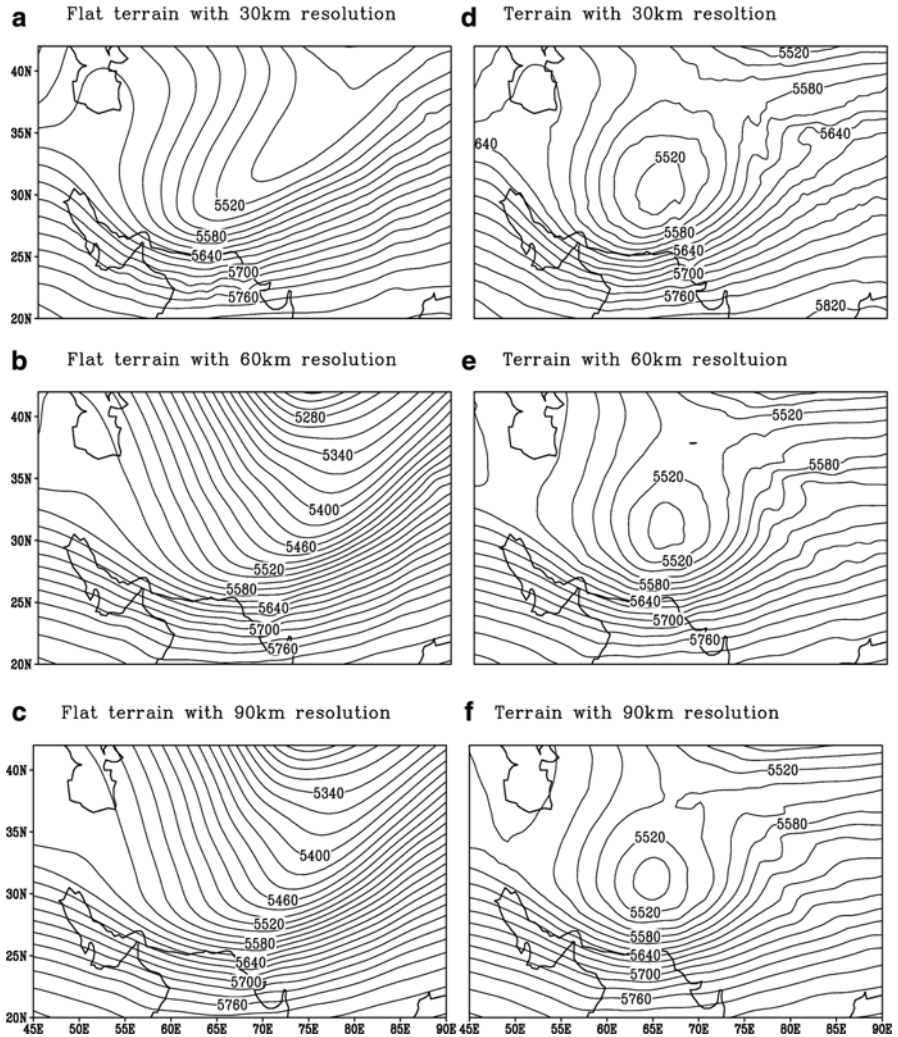


Fig. 2.3 500 hPa Geopotential height (m) after 48 h model forecast valid at 0000 UTC on 23 Jan 1999 over flat (a, b and c) and normal topography (d, e and f) with different model horizontal resolutions

showed that the same model could not accurately capture the advection during a WD and thus failed to simulate the observed speed of the system.

The associated intensification and modulation of the WD is further illustrated in Fig. 2.5a using results of WRF model simulations for the WD on 7 Feb 2002 and compared with the corresponding reanalyses results. Figure 2.5a depicts model-simulated 500 hPa wind, geopotential height, and wind speed which show similar cyclonic structure as in the corresponding with two reanalyses results presented in Fig. 2.5b and c respectively. The two reanalyses datasets are - Modern Era

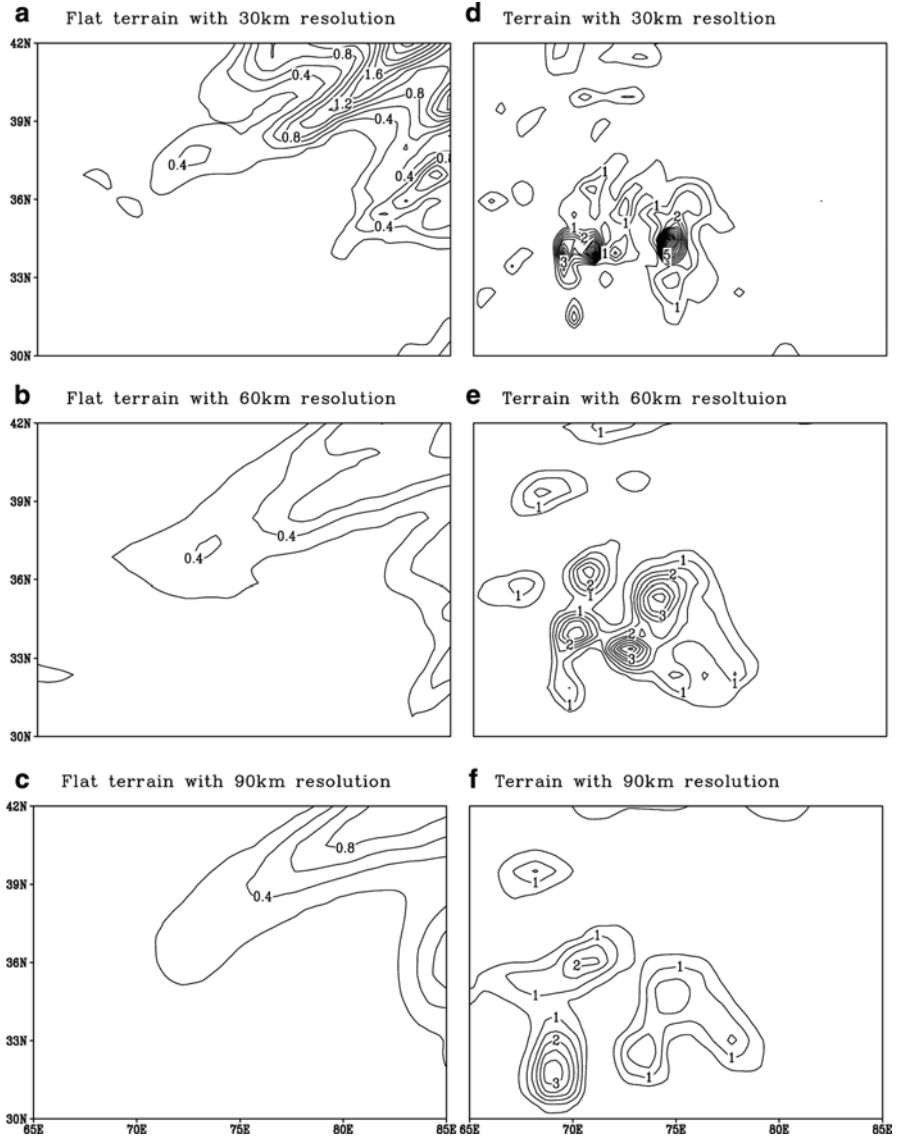


Fig. 2.4 Precipitation (cm/24 h) after 48 h model forecast valid at 0000 UTC on 23 Jan 1999 over flat (a, b and c) and normal topography (d, e and f) with different model horizontal resolutions

Retrospective Analysis for Research and Applications (MERRA) and National Center for Environmental Prediction – National Center for Atmospheric Research Reanalysis Project (NCEP-NNRPII). The wind speed shown in the shaded grey region depicts the flow intensifying along the cyclonic circulation. The overall wind pattern indicates that the model could simulate anomalous cyclonic circulation as

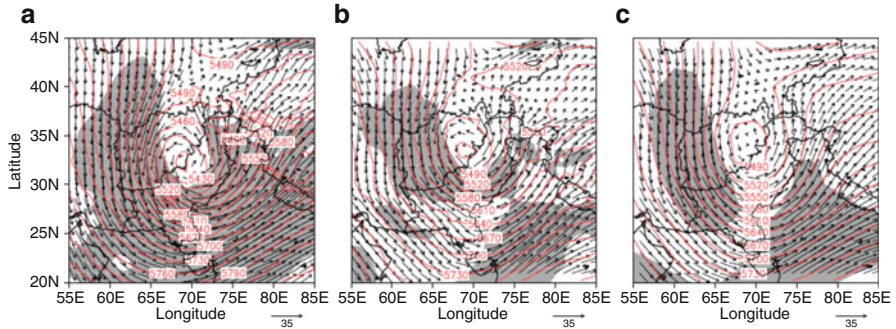


Fig. 2.5 500 hPa wind (m/s; arrow); geopotential height (m; red contour) and wind speed above 22 m/s (grey shed) in (a) model, (b) MERRA and (c) NCEP-NRPII on 07 Feb 2002 0000 UTC

seen in the corresponding verification analysis with higher magnitude. The corresponding geopotential field corroborates with the mid-tropospheric trough over the Indo-Pak region. The figure depicting model-simulated geopotential height is similar to the corresponding observational reanalysis. The trough/depression is depicted over Pakistan and north-west India which forms the cyclonic circulation. Correspondingly, the model also shows the high wind speeds due to the stronger storm simulation. The well-marked low developed over the region, and movement of the said low pressure system is depicted well in the model simulation. The model simulates a more intense storm, thus, over predicting all associated fields leading to stronger cyclonic circulation and stronger wind speed in comparison with the observation data. Corresponding thermodynamical factors, maximum convective available potential energy (CAPE) and convective instability (CINE) are presented in Fig. 2.6a and b respectively. It depicts the spatial distribution of CAPE and CINE on 7 February 2002 elongated along the Himalayan topography. These figures show that during passage, the WD interacts with topography generating enough energy for intensification of the winter storm, thus enhancing associated precipitation over northern India. Such interplay of the WD with topography provides an explanatory inference for the propensity of increased weather activity (Dimri and Niyogi 2012). Increase in CAPE is the release of energy from the instability in the atmosphere that is associated with the orographic lifting of unstable moist air. The kinetic energy generated through conversion of CAPE maintains the convective system during the WD occurrence. During the peak of the WD, CAPE provides support for intensification, which over time reduces significantly the dissipation of the energy and thus weakens the WD. Similarly there is also an increase in the CINE as seen in the figure across the region of WD occurrence. Though this parameter acts as an inhibiting agent for convection, the higher values of CAPE promote the WD. The high values of CINE in a region of high CAPE values indicates the development of the synoptic system in the vicinity. Overall there clearly is an increase in the values of CAPE and CINE in correspondence to the occurrence of precipitation.

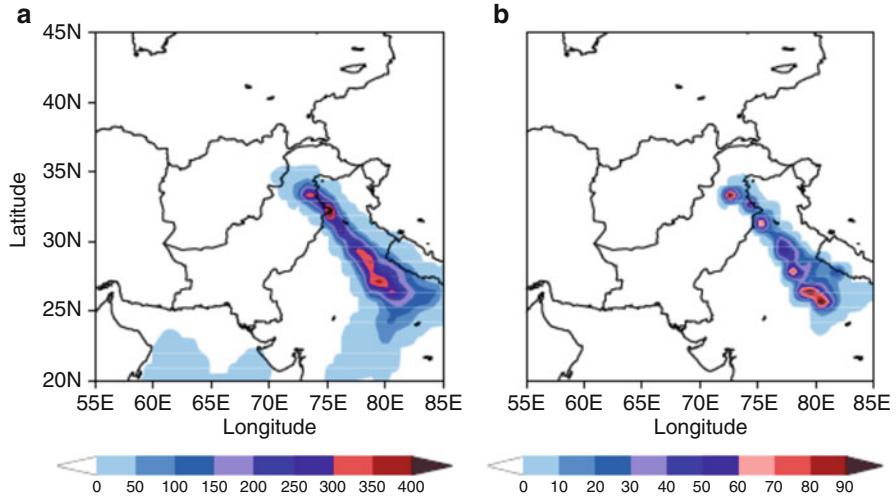


Fig. 2.6 Spatial distribution of model simulated maximum (a) CAPE (J/kg) and (b) CIN (J/kg) on 07 Feb 2002 0000 UTC

Roy and Bhowmik (2005) observed similar high values of CAPE and CINE associated with the days of occurrence of precipitation during WDs.

Another study by Chevuturi et al. (2014) was intended to analyse winter hailstorms over India using numerical weather prediction. This is still under the purview of our book as the study reported that the winter hailstorm was caused by the presence of a WD. Hailstorms are highly convective events and are uncommon during the cold and dry winter months. But this study describes how winter hailstorms are caused by the WD and in turn also provides a detailed description of the baroclinic conditions developed during a WD. We have mentioned the baroclinicity associated with the WDs before as described by Singh and Agnihotri (1977), but in this section we will describe the condition in much greater detail as per the study of Chevuturi et al. (2014). In the study, the vertical cross section of the field variable along the axis of core precipitation zone of the storm is shown in Fig. 2.7. The area-averaged values over the $1^\circ \times 1^\circ$ grid around the region of peak precipitation is shown in Fig. 2.8. The region over and around 77.2° E and 28.6° N would be considered the NCR (national capital region/New Delhi) or the region of study/interest. Over NCR the geopotential height anomaly shows an increase around 400–200 hPa (Fig. 2.7). This increase is associated with the dipping in the perturbation geopotential height contour lines. These changes are due to the tropopause fold penetrating the troposphere. The dip in the tropopause height values is also observed in the station data over New Delhi. This tropopause lowering is associated with baroclinic instability occurring over the region (Bush and Peltier 1994). The increased storm intensity over the region is caused by the baroclinic instability due to the passing WD and the development of cyclonic circulation. The mid-latitude migratory WD attains higher intensities in the form of a baroclinically unstable disturbance specifically over the

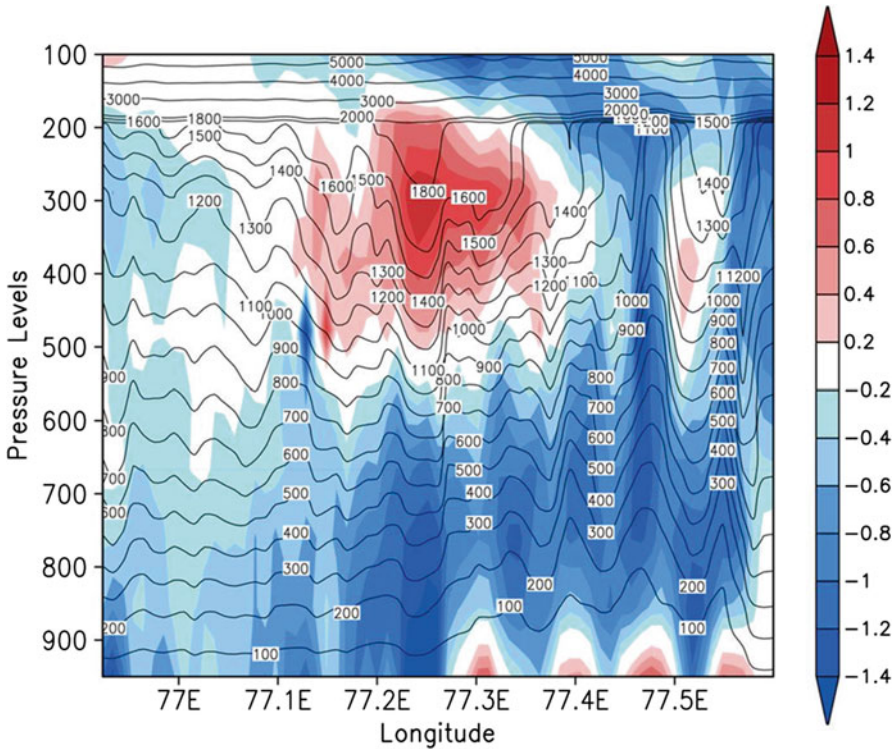


Fig. 2.7 Longitude-pressure cross section (at the line across peak precipitation spatial distribution of the storm) at 1700 UTC 17 Jan 2013 for geopotential height anomaly (*shaded*) and perturbation geopotential height (m; *contour*)

Indian region (Rao and Rao 1971; Singh and Agnihotri 1977). This instability in the mid- to upper-tropospheric levels generates the turbulent convective energy required for the development of updrafts during storm occurrence. With the availability of moisture in the atmospheric column, the instability leads to heavy precipitation. This is the usual baroclinic condition associated with a WD. While not all WDs over northern India lead to hail formation during winter, some of the intense WDs may lead to the hail formation. Heymsfield et al. (2005) describes how strong convective updrafts (with vertical wind speed greater than 5–10 m/s) suppress homogenous nucleation to form the ice particles which grow to form hail. However, lower wind speeds would not contain enough energy to develop a strong hailstorm. In cases of WDs occurrences where such updrafts are, the hail formation may be possible over northern India. The instability developed in the mid-tropospheric levels due to the WD increases the propensity for baroclinic atmosphere in the upper half of the troposphere. When the temporal variation of temperature profile of the region is analysed, a dip is observed in the $-60\text{ }^{\circ}\text{C}$ isotherm around 1600–1700 UTC (Fig. 2.8). This lowering corresponds to the tropospheric fold discussed before.

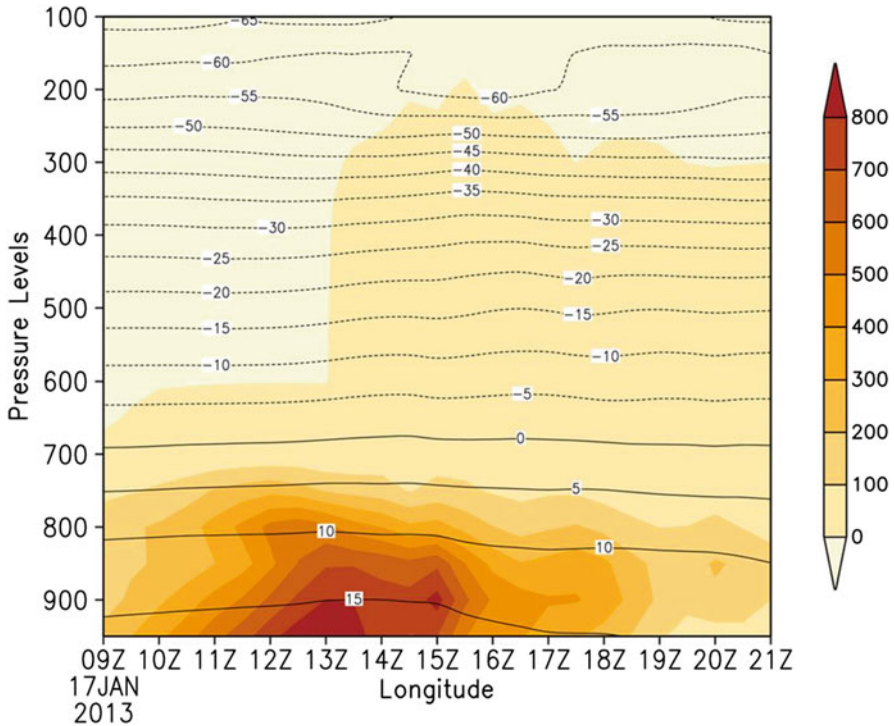


Fig. 2.8 Time-pressure cross section (area averaged over the grid around NCR) for CAPE (J/kg; shaded), temperature ($^{\circ}\text{C}$; black contours) and specific humidity (g/kg; blue contours)

The lowering in the tropopause causes the incursion of colder stratospheric layers into the warmer troposphere. This in turn causes development of a steep temperature gradient as seen in the figure, which enhances upper-level instability. Still the reasons for instability in the lower layers are yet not clearly addressed. To understand the lower layer instability, temporal variation in area-averaged CAPE and specific humidity are represented in the black and blue contours of Fig. 2.7 respectively. In this figure, an increase of moisture over NCR in the lower levels of the atmospheric column is observed along with development of CAPE from around 1300 UTC. The source of this low-level moisture incursion is primarily from the Arabian Sea and, to a lesser extent from the Bay of Bengal. The moisture convergence develops buoyancy which enhances the propensity of increase of CAPE in the atmospheric column. There is reduction in CAPE values in subsequent time periods after 1300 UTC. The increase of CAPE defines the potential energy that is available to drive a storm and release of CAPE in the form of kinetic energy promotes storm development. Along with this, the low-level moisture incursion provides the buoyancy required for the air parcel to rise. Thus, upper-level baroclinic instability is due to the presence of the WD embedded within the SWJ.

Various other studies examined the sensitivity to model the physics, spatial horizontal-model resolution, topography, domain, etc. towards the representation of WDs, and exhibited a systematic bias with the error in WD simulation increasing with integration time (Dimri and Mohanty 2009). These model biases can be reduced through the assimilation of satellite-derived atmospheric temperature profiles (Rakesh et al. 2009), surface observations (Dasgupta et al. 2012), and improved boundary conditions such as land-use maps (Thomas et al. 2013). This combination has provided significant improvement in the simulated precipitation intensity and dynamics associated with WD dynamical evolution from the forecasters' point of view and also the control factor of complex Himalayan topography within the model physics (Semwal and Dimri 2012). Accurate real-time prediction of WDs, which result in heavy snowfall and gale speed winds, allows for timely warnings of avalanches and landslides (Srinivasan et al. 2005). Dimri and Ganju (2007) and Dimri (2009) analysed the impact of orography and land-use interaction during mesoscale simulations using a regional climate model for WD simulation. Das et al. (2003) and Das (2005) were studies specifically directed to mesoscale modelling for forecasting of WDs over mountainous regions. These two studies identified model details for improved accuracy of mountain weather forecasting over the Indian region. Performance of the operational global circulation model called T80, used at National Centre for Medium Range Weather Forecasting (NCMRWF) for forecasting WDs, has also been studied (Gupta et al. 1999). They analysed four WD cases in detail to study the performance of the model for various qualitative and quantitative variables. The study showed an overall fair performance of the model, but still there was under prediction of the heavy precipitation event.

Even with some short-comings, there has been a marked improvement in the understanding of model simulation strategies in recent decades. This has enabled assessment of WD structure and dynamics with a level of detail that was very elusive earlier. These enhancements and improvements over time have been tabulated in the Table 2.1. These studies in the future will help forecasters in assessing these factors in advance through modelling efforts. Though there have been improvements, most studies still demonstrate deficiency in WD forecasting. Improvements have been suggested in the form of improved parameterization schemes specific for the mountainous regime of the Himalayas where the WDs occur. Improvements in developing a better observational network over this region, which has paucity of data, can improve the understanding of the weather systems impacting the region.

2.3 Interplay With Himalayan Orography and Land-use – Land-Cover Interactions

From the discussions in the previous and the current chapter, we can say that surface interactions have a significant impact on the extra-tropical systems, the WDs. Two types of surface interactions of WDs will be discussed in this section. The first is the

interaction with the orography or the height variability of the surface. Orography acts as a barrier to the circulation patterns and weather systems and so has a significant impact on their dynamics. The second is the interaction with variability in the land-use and land-cover patterns over the region impacted by the WDs. Land-surface interactions have more of a thermodynamical impact on the atmosphere above them. Overall these two interactions have a significant impact on not only the origin and structure but also the movement and intensity of the WDs.

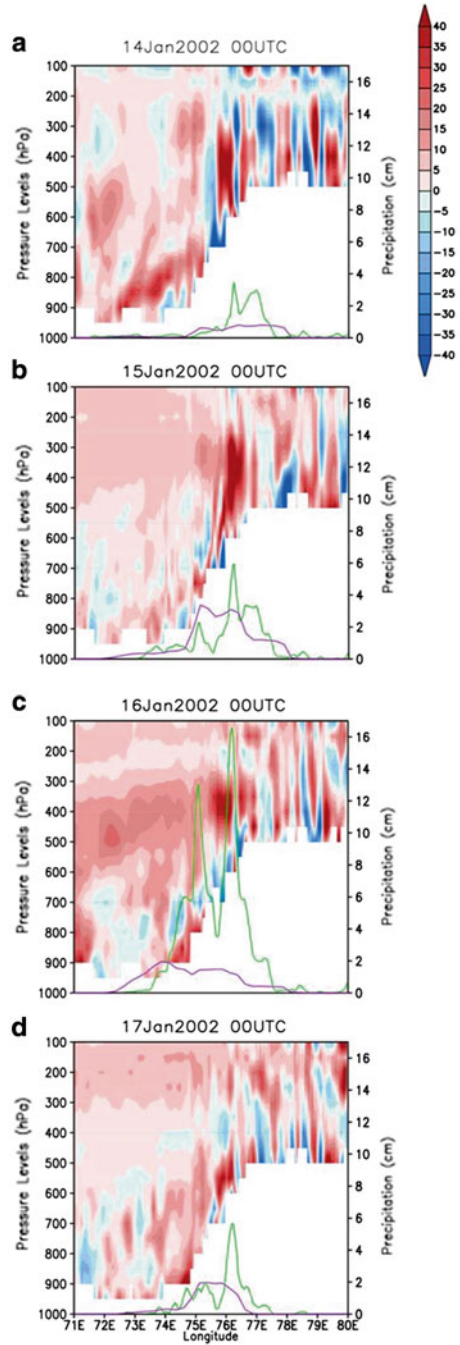
The first influence of orography is during the origin and migration of the WDs. After the formation of the depressions in the eastern Mediterranean, as these approach the highlands of Iran these systems break into two (Mull and Desai 1947). Their first portion moves north-eastwards towards northern Iran and is termed primary. Whereas the second portion moves over the Persian Gulf and southern Iran and is termed the secondary. This part of the depression is what ultimately forms the WDs that impact India. Though, this term secondary should not be confused with the secondaries of the induced WDs which have been discussed previously. The tendency of the parent depression to break up into the two depression due to the Iran Highlands is specific during winters since the SWJ lies over the region during this season. Further, during the migration of the depressions eastward, there is the possibility of orography influencing the structure of the WDs. Pisharoty and Desai (1956) reported that the weather systems that start out as frontal systems arrive over India in an occluded state without the frontal structure in the lower levels but the structure maintained in the higher levels of atmosphere. The rough orography of Iran, Afghanistan and Western Pakistan remove the frontal structure from the lower levels of this system due to friction. The distribution of orography within the path of the WD system tends to develop the secondaries as discussed before (Malurkar 1947). According to Mull and Desai (1947), as the depression center crosses near a mountain range, the cold front gets cut off from the warm front and the development of secondaries is possible. But for the orography to impact the WD depression, it is required that the system is sufficiently close to the mountain. A head-on interaction of the orography with the migrating depression may cause the depression to completely collapse if the depression height is lower than that of the mountain. Whereas if the height is higher, the lower portion of the depression is eroded (Mull and Desai 1947; Pisharoty and Desai 1956). This causes the reduction in the kinetic energy of the system which revives with the influx of fresh warm and moist air in the lower levels. This forms the occluded structure of the WD, with the frontal depression in the upper levels and low level buoyancy due to the moist-air incursion.

The final impact of orography on the WDs is the impact the Himalayas have on the WDs when the weather systems finally arrive over India and interact with the mountain range. The interplay of WDs with the topography of the Western Himalayas determines spatial and vertical distribution of precipitation. According to Dash et al. (2009), the rest of the Indian region receives most rainfall during monsoons but northwestern India receives up to 15 % of its annual precipitation during the winters and this is related to the interaction of WDs with the orography (Yadav et al. 2012). The annual precipitation pattern derived from Tropical Rainfall Measuring Mission (TRMM) satellite radar data shows gradients across the range,

from east to west, and fivefold differences between major valleys and their adjacent ridges (Barros et al. 2000; Lang and Barros 2002; Anders et al. 2006). Dimri and Chevuturi (2014) reported that the precipitation patterns associated with the WDs showed an axis along the Himalayan orography. The interannual variability of precipitation in the Nepal region of the Himalayas is dependent on the timing of the summer monsoon onset along the Himalayan range and is linked to the trajectories and strengths of the monsoon depressions forming over the Bay of Bengal (Lang and Barros 2002; Barros et al. 2006). Lang and Barros (2004) defined the WDs as “*westerly waves trapped and intensified by the unique large-scale topographic features, most notably the notch formed by the Himalayas and Hindu Kush mountains*”. The interannual variability of these systems is high and is dependent on the intensity of the circumpolar westerly jet and the location of the incoming disturbance with respect to the Tibetan Plateau. They also reported that orographic forcing is the dominant factor maintaining the precipitation due to WDs over the Himalayas. Evolution of the large-scale flow into an accurate geometric formation with respect to the orography causes significant precipitation over the region. Similarly, the orientation of major drainage basins and catchment areas can also lead to local differences in the distribution of precipitation (Barry 2008). The upper-level flow may interact with topography in variable ways to affect the low-level cloud motion in the valley. The precipitation to cloudiness scaling suggests a strong stationary behavior of orographic land-atmosphere interactions based on elevation class and ridge-valley scales (Barros et al. 2004). This is to be expected as topography plays a crucial role in modifying these WD weather systems (Dimri 2004). This study analysed the sensitivity of model simulation of WDs with horizontal model resolution. The reports suggested that finer resolutions simulate precipitation better as, at finer resolutions, the orographic effect and corresponding sub-grid mesoscale forcing are better represented within the model. Similar studies of Mohanty and Dimri (2004), Dimri (2009); Dimri and Mohanty (2009) described topographic interaction of WD cyclonic circulation and Himalayan orography. According to the studies, in the Himalayan mountainous region, the precipitation is location specific and dependent on the orography. Raju et al. (2011) studied the role of the Himalayan orography in blocking and guiding the integrated moisture fluxes during an active WD occurrence, as previously discussed. Though the Himalayas block the winter storms and cause precipitation on the windward side, exceptionally violent rainstorms can overcome orographic barriers and penetrate far into otherwise arid regions in the northwestern Himalayas at elevations above 3000 m (Bookhagen et al. 2005). Otherwise, in general, blocking effects prevail and penetration occurs along river valleys or mountain passes (Barros et al. 2006). Winter depressions are either strongly blocked or deflected by the Himalayan topography.

Orographic forcing of the Himalayas on the WDs has also been studied by Dimri and Chevuturi (2014) using a numerical simulation method. Figure 2.9 shows the vertical cross-sectional distribution of vorticity and precipitation along with topography across 33°N for a WD during January 2002. Here increased positive vorticity is observed over and along upslope orography particularly at 76.5° E from 14 January 2002 to 16 January 2002. Intensification of cyclonic circulation is associ-

Fig. 2.9 Vertical cross section of vorticity ($\times 10^5 \text{ s}^{-1}$, *shaded*), model precipitation (cm/day; *green line*) and observed precipitation (cm/day; *purple line*) along 33°N for the WD case studied

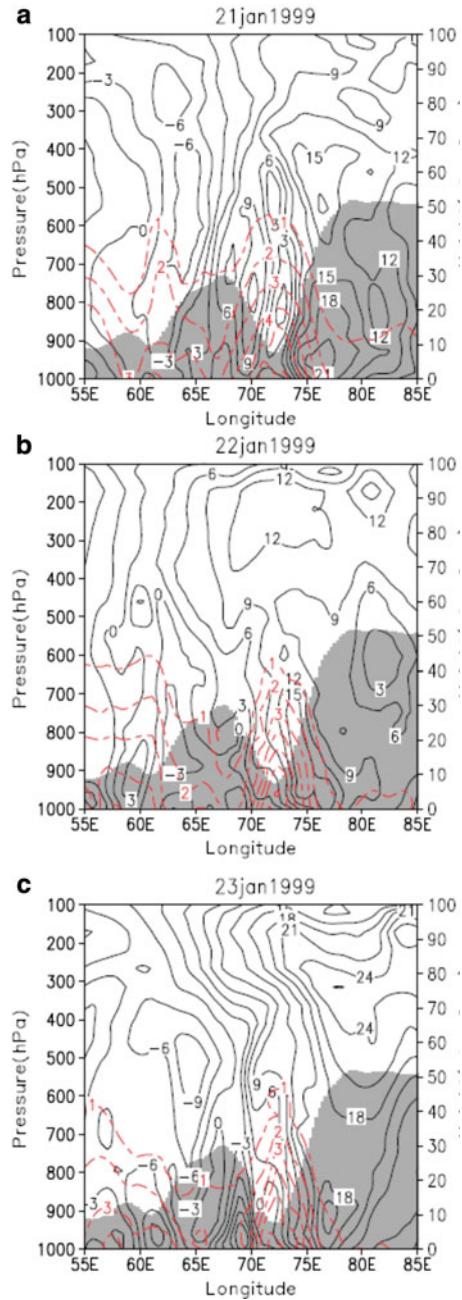


ated with increased positive vorticity, which in turn will intensify the WD and hence increase associated precipitation. It is also clearly seen that positive vorticity is closely associated with the maxima of precipitation. The distribution of vorticity along the rising topography of the Western Himalayan region causes the orographic forcing producing the precipitation by the WDs. It is seen that upslope increased cyclonic vorticity corresponds to increased precipitation which could be seen in increased precipitation in model fields and observation fields as well. Though quantitatively precipitation fields differ, their distribution along the topographic upslope and/or downslope is similar. This figure illustrates the precipitation forming mechanism along the upslope topography. There is also formation of an associated positive vertical wind flow along the topography which causes the rising air parcel. The increased vertical-velocity associated increase convective activity is noted along the region which further forms clouds and causes precipitation. Similar positive vorticity along the orography of the Himalayas during a WD occurrence was reported by Hara et al. (2004).

WD model simulations show that the implementation of a sub-grid land-use scheme leads to a more realistic simulation of precipitation and surface air temperature (Dimri 2009). The sub-grid scheme provides a more accurate representation of resolvable sub-grid-scale processes and atmospheric/surface circulations that result in a better representation of the storm. With a set of modelling experiments, Dimri and Niyogi (2012) provided insight into the interplay of topographic and WD circulation during the 21–23 January 1999 case. Figure 2.10a, b and c presents a longitude and vertical cross sectional distribution of meridional wind and air specific humidity at 34°N latitude at 0000 UTC on 21, 22 and 23 January 1999 respectively. This cross section was chosen because the highest topographic variability is seen across this latitude. Higher vertical wind shear in the lower troposphere and stronger meridional wind from the surface to 500 hPa along the Kashmir valley (~73° E) is discernible during the WD event. Also, contrast in meridional winds from the surface to 200 hPa is seen around ~67° E. Along the valley topographic boundaries, the wind is weaker, while in the middle of the valley, the wind is stronger. Also, an increase in air-specific humidity up to the mid-troposphere over the valley is clearly visible, which is lower along the valley topographic slopes/boundaries.

To investigate the precipitation mechanisms associated with WDs, a case during 20–22 December 2006 was investigated by Dimri et al. (2013). They documented the distribution of moisture variables and vorticity modulation due to topography in the intensification of WD. The Asian Precipitation -- Highly Resolved Observational Data Integration Towards Evaluation of the Water Resources (APHRODITE; Yatagai et al. 2012) (for the 24-h cumulative at 0000 UTC on 22 December 2006) shows a large daily precipitation event (see Fig. 2.11a). Note that the western Himalayan region has a limited observational network and most of the available reanalyses are based on the assimilation of satellite measurements, upper-air observations, and limited ground observations. Furthermore, the number of stations per grid cell is available for APHRODITE. This information was used to determine to what extent the gridded precipitation was determined from station data or derived using an interpolation between the stations. The climate over the western Himalayas

Fig. 2.10 Lon-pressure cross section vertical distribution at 34°N latitude of model simulated meridional wind (ms^{-1}) (continuous *black contour*) and air specific humidity ($\times 10^{-3}$) (broken *red contour*) at 0000 UTC during active WD **(a)** 21 Jan 1999 **(b)** 22 Jan 1999 **(c)** 23 Jan 1999 (*Left hand side* vertical axis corresponds to the pressure distribution and *right hand side* vertical axis corresponds to the topography $\times 10^2$ m)



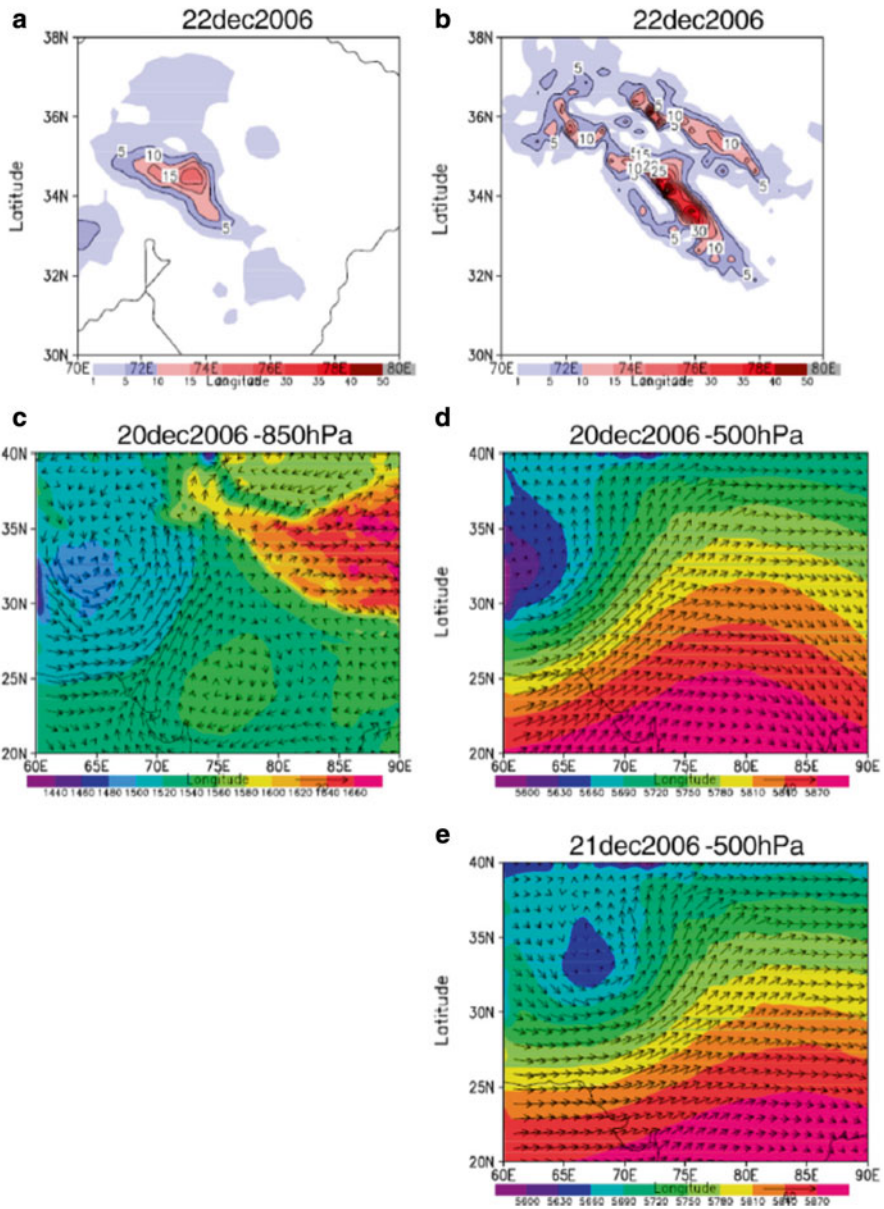


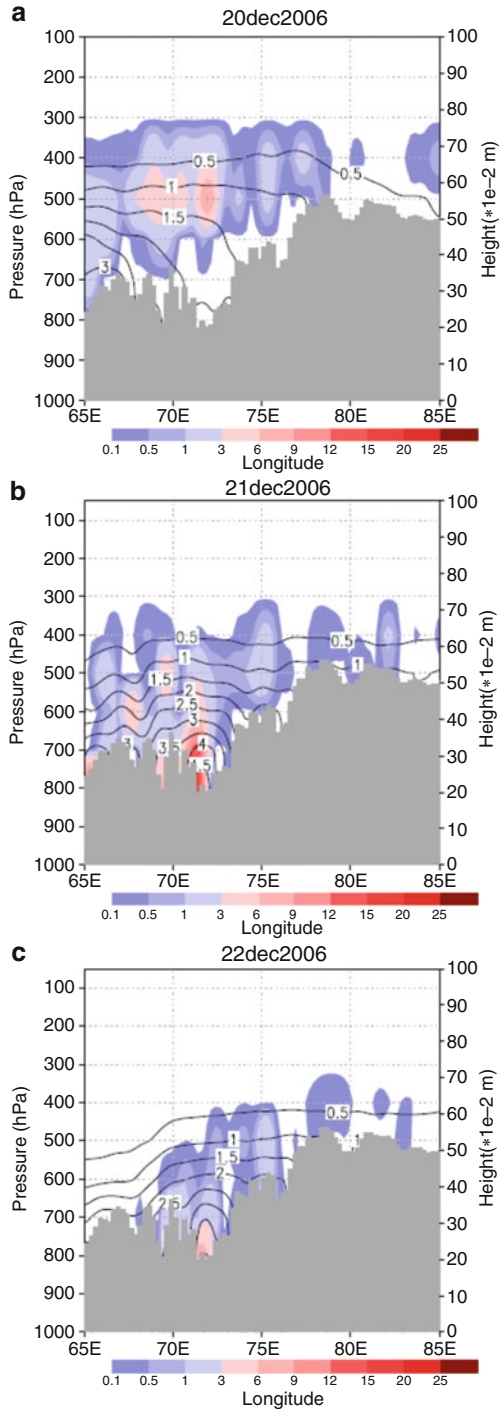
Fig. 2.11 Twenty-four hour cumulative precipitation on 22 December 2006 in (a) observational data (APHRODITE) and (b) the corresponding REMO simulated field, and geopotential height (m; *shade*) and vector wind (m/s; *arrow*) in the REMO simulation at (c) 850 hPa on 20 December 2006, (d) 500 hPa on 20 December 2006, and (e) 500 hPa on 21 December 2006

is colder and drier than that of other Himalayan regions, and therefore the daily time resolution of APHRODITE is more reliable than the monthly time resolution of other datasets and is, to date, the finer precipitation reanalysis available (25 km resolution). Also representation of vertical and horizontal discretization of topography in the analytical methodology makes this dataset comparably better than other observational reanalysis as it inputs the role of topography while preparing the reanalysis. The simulated precipitation from the Regional Climate Model (RCM)–REMO (Jacob et al. 2007) for this event is shown in Fig. 2.11b. The model simulation uses global ERA-Interim reanalysis data (Dee et al. 2011) to supply large-scale boundary conditions (LBCs). REMO uses the GTOPO30 topography data of the US Geological Survey (USGS). The domains were chosen to cover the whole area of India including the Himalayas. REMO RCM simulated the regional climate with a spatial resolution of 0.23° (~ 25 km). Such model resolution was chosen to match APHRODITE resolution. In the model and the corresponding observation, the peak precipitation appears across the Himalayan range, with the model showing the wet bias. The RCM geopotential height field at 850 hPa (Fig. 2.11c) shows a well-defined surface low associated with cyclonic circulation over 33°N , 65°E in the northwest of the western Himalaya two days earlier. The system develops on 20 and 21 December 2006 as it moves over the western Himalaya (Fig. 2.11d and e), indicating that such systems can be adequately depicted from the RCM's simulation. Figure 2.12 illustrates the vertical distribution of geopotential anomaly and specific humidity during that period. The clear influence of the topographic valley floor, upslopes, and downslopes are discernible in defining the spatial organization of precipitation.

The vorticity and relative humidity distribution over this period are presented in Fig. 2.13. The vertical deflection of flow induced by the topography results in adiabatic cooling, and, if sufficient moisture is available from clouds, will eventually lead to precipitation. Convergence on the upslope/windward side due to decreased velocity through orographic retardation will deform or slow down the flow, generating a mid-troposphere positive vorticity at the peak of the storm (Fig. 2.13a and b). Higher relative humidity is seen in the regions of positive vorticity (Fig. 2.13b and c). A weaker negative vorticity occurs along the topographic surface toward the windward side with positive vorticity over the leeward side and over the valley floors. The effects of stronger valley flows are twofold: first, these stronger valley flows reduce upslope moisture flow by channeling it, and second, the lateral circulations constrained by the valley boundaries provide conditions for precipitation formation. This suggests the models' robustness for mountainous regions at the event scale.

Important mountainous physical processes that need an explicit driving mechanism in the model physics are discussed and deliberated in Barros and Lettenmaier (1994), Leung and Ghan (1995) and Bindlish and Barros (2000). Barros and Lettenmaier (1994) had shown earlier efforts of modelling and certain type of precipitation over mountains and associated runoff. Lin et al. (2001) has shown

Fig. 2.12 Lon-pressure cross section vertical distribution at 34°N latitude of model simulated geopotential height (m; *continuous black contour*) and air specific humidity ($\times 1e-3$; *shaded*) at 0000 UTC during active WD (a) 20 Dec 2006 (b) 21 Dec 2006 (c) 22 Dec 2006 (*Left hand side* vertical axis corresponds to the pressure distribution and right hand side vertical axis corresponds to the topography $\times 10^2$ m)



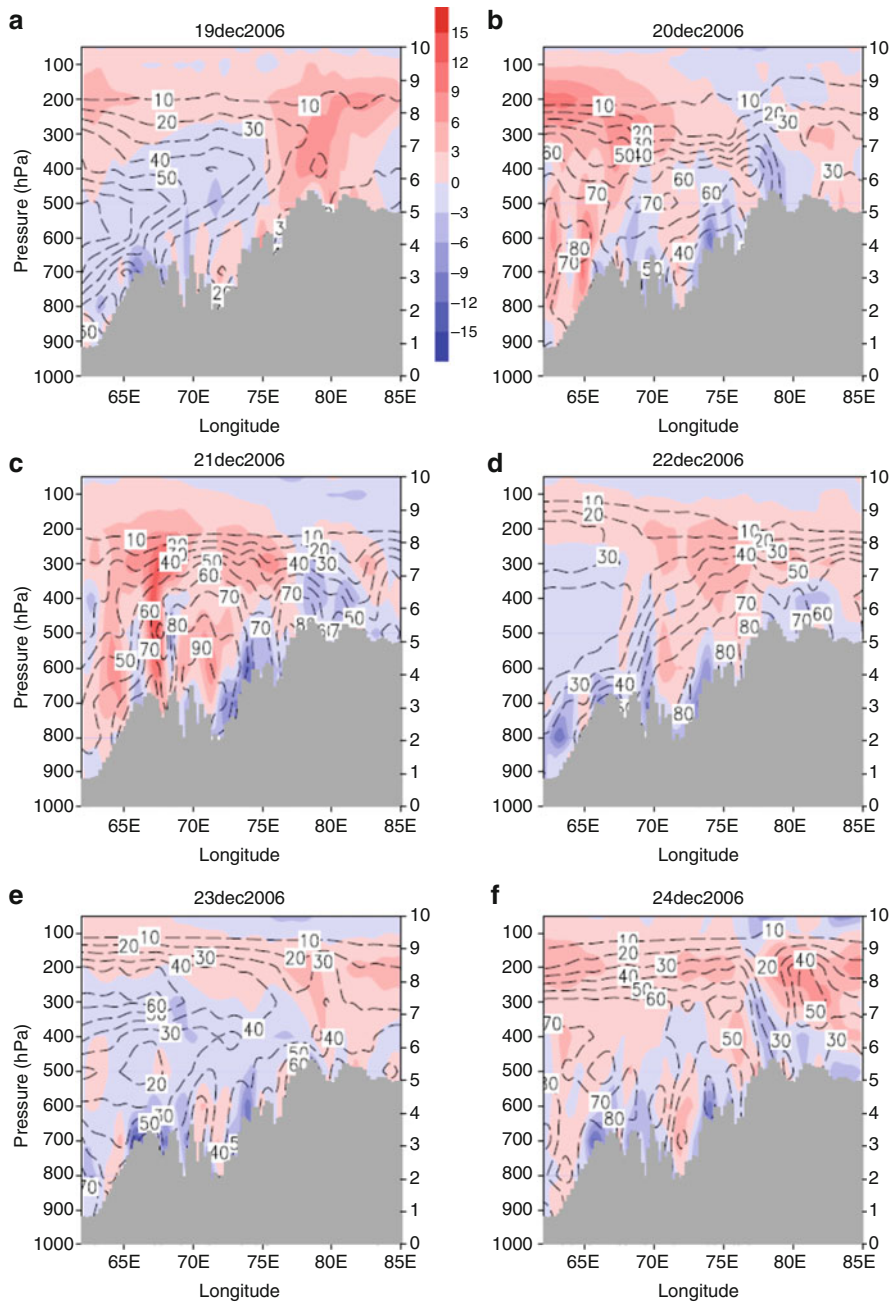


Fig. 2.13 Lon–pressure distribution of vorticity ($\times 1e-5/s$; *shade*), relative humidity (%; *broken contour*), and topography ($\times 10^3$ m; *shaded bar*) on (a) 19 December 2006, (b) 20 December 2006, (c) 21 December 2006, (d) 22 December 2006, (e) 23 December 2006, and (f) 24 December 2006 at 35°N Lat in the REMO simulation

environmental controls favoring heavy precipitation events over the mountainous regions. A theoretical framework of influence of stable moist airflow on precipitation over the mountains and its formulation in the idealized model condition is reviewed and proposed by Smith (2006). Roe (2005, p. 665) provided holistic review of the precipitation mechanism over mountains: ‘orographic precipitation is intrinsically a transient phenomenon, It tends to occur during the passage of a pre-existing weather disturbance, and precipitation rates can vary substantially during the course of a single storm as a synoptic conditions change...’. This review gave an insight about the orographic interaction and precipitation mechanism over the mountains. The most recent review by Houze Jr (2012, p. 42) has provided the latest insight into the orographic precipitation mechanism. ‘It provided variety of orographic effects that profoundly modify the structure of major precipitating cloud systems through combinations of dynamical response, terrain shape and size, and alteration of microphysical timescales...’.

The influence of various sections of the Tibetan Plateau and orography (referred as ‘regional mountain uplift’) is proposed by Chakraborty et al. (2002). He suggested that the presence of the western Tibetan Plateau is more instrumental to the formation of ISM than the eastern Tibetan Plateau. Boos and Kuang (2010) illustrated that the presence of the Himalayan orography and adjacent mountains sustain the present day strength of ISM. There is an important finding that the orographic insulation of low-entropy *extra-tropical air masses by the narrow mountain chains* (i.e. ‘thermal insulation’) rather than the diabatic heating of the entire elevated plateau maintains the ISM (Tang et al. 2013).

The above discussion is focused on the impact on the WDs themselves of the interactions between WDs and surface. These interactions might also have an impact on the orography and land surface. These impacts will be separately elucidated in the last chapter of this book.

References

- Agnihotri CL, Singh MS (1982) Satellite study of western disturbances. *Mausam* 33(2):249–254
- Agnihotri CL, Singh MS (1987) Absorption of short-wave radiation in the atmosphere over India in winter. *Mausam* 38(1):79–84
- Agrawal KC (1999) An introduction of avalanche forecasting and future trends. In: Dash SK, Bhadur J (eds) *The Himalayan environment*. New Age International Pvt. Ltd, New Delhi, pp 71–78
- Ananthkrishnan R, Keshavmurthy RN (1973) A preliminary study of the adiabatic generation and dissipation of kinetic energy by meridional and zonal winds over India and neighborhood during winter seasons. *Indian J Meteorol Geophys* 24:235–244
- Anders AM, Roe GH, Hallet B, Montgomery DR, Finnegan NJ, Putkonen J (2006) Spatial patterns of precipitation and topography in the Himalaya. In: Willett SD, Hovius N, Brandon MT, Fisher DM (eds) *Tectonics, climate, and landscape evolution*. Geological Society of America Special Papers 398, pp 39–53
- Azadi M, Mohanty UC, Madan OP, Padmanabhamurty B (2001) Prediction of precipitation associated with western disturbances using a high-resolution regional model: role of parameterisation of physical processes. *Meteorol Appl* 7:317–326

- Azadi M, Mohanty UC, Madan OP (2005) Performance of a limited area model for the simulation of western disturbances. *J Aerosp Sci Technol* 2(2):29–35
- Bamzai AS, Shukla J (1999) Relation between Eurasian snow cover, snow depth and the Indian summer monsoon: an observational study. *J Clim* 12:3117–3132
- Barros AP, Lettenmaier DP (1994) Dynamic Modeling of Orographically-Induced Precipitation. *Rev Geophys* 32:265–284
- Barros AP, Joshi M, Putkonen J, Burbank DW (2000) A study of 1999 monsoon rainfall in a mountainous region in central Nepal using TRMM products and rain gauge observations. *Geophys Res Lett* 27:3683–3686
- Barros AP, Kim G, Williams E, Nesbitt SW (2004) Probing orographic controls in the Himalayas during monsoon using satellite imagery. *Nat Hazards Earth Syst Sci* 4:29–51
- Barros AP, Chiao S, Lang TJ, Burbank D, Putkonen J (2006) Tectonics, climate, and Landscape Evolution. In: Willett SD, Hovius N, Brandon MT, Fisher DM (eds) Tectonics, climate, and landscape evolution, Geological Society of America Special Paper 398. Geological Society of America, Boulder, pp 17–28
- Barry RG (2008) Mountain weather and Climate. Cambridge University Press, New York
- Bindlish R, Barros AP (2000) Disaggregation of rainfall for one way coupling of atmospheric and hydrological models in regions of complex terrain. *Glob Planet Chang* 25:111–132
- Bookhagen B, Thiede RC, Strecker MR (2005) Abnormal monsoon years and their control on erosion and sediment flux in high, arid northwest Himalaya. *Earth Planet Sci Lett* 231:131–146
- Boos WR, Kuang Z (2010) Dominant control of the South Asian monsoon by orographic insulation versus plateau heating. *Nature* 463:218–222
- Bush ABG, Peltier WR (1994) Tropopause folds and SynopticScale Baroclinic wave life cycles. *J Atmos Sci* 51:1581–1604
- Chakraborty A, Nanjundiah RS, Srinivasan J (2002) Role of Asian and African orography in Indian summer monsoon. *Geophys Res Lett* 29(20):50–1–50–4. doi:10.1029/2002gl015522
- Charney JG (1947) The dynamics of long waves in a baroclinic westerly current. *J Meteorol* 4:135–162
- Charney JG (1948) On the scale of atmospheric motions. *Geophys Publ* 17(2):1–17
- Charney JG, Fjørtoft R, Von Neumann J (1950) Numerical integration of the barotropic vorticity equation. *Tellus* 2:237–254
- Chevuturi A, Dimri AP (in review) Investigation of Uttarakhand (India) disaster- 2013 using Weather Research and Forecasting model
- Chevuturi A, Dimri AP, Gunturu UB (2014) Numerical simulation of a rare winter hailstorm event over Delhi, India on 17 January 2013. *Nat Hazards Earth Syst Sci* 14(12):3331–3344
- Chitlangia PR (1976) Mean model of western depression. *Indian J Meteorol Hydrol Geophys* 87(2):157–162
- Das S (2002) Evaluation and verification of MM5 forecasts over the Indian region. In Proceedings of 12thPSU/NCAR mesoscale model users workshop, Colorado, pp 77–81.
- Das S (2005) Mountain weather forecasting using MM5 modelling system. *Curr Sci* 88(6):899–905
- Das S, Singh SV, Rajagopal EN, Gall R (2003) Mesoscale modeling for mountain weather forecasting over the Himalayas. *Bull Am Meteor Soc* 84:1237–1244
- Dasgupta M, Das S, Ashrit R (2012) MM5 3D-Var data assimilation and forecast system over Indian Subcontinent – results from recent experiments. <http://www.mmm.ucar.edu/mm5/workshop/ws04/Session5/Gupta.Das.pdf>. Accessed on 19 Mar 2013
- Dash SK, Chakrapani B (1989) Simulation of a winter circulation over India using global spectral model. *Earth Planet Sci* 98(2):189–205
- Dash SK, Jenamani RK, Kalsi SR, Panda SK (2007) Some evidence of climate change in twentieth-century India. *Clim Chang* 85(3–4):299–321
- Dash SK, Kulkarni MA, Mohanty UC, Prasad K (2009) Changes in the characteristics of rain events in India. *J Geophys Res* 114(D10109):1–12

- deSilva AM, Lindzen RS (1993) On the establishment of stationary waves in the Northern Hemisphere winter. *J Atmos Sci* 50:43–61
- Dee DP, Uppala SM, Simmons AJ, Berrisford P, Poli P, Kobayashi S, Andrae U, Balmaseda MA, Balsamo G, Bauer P, Bechtold P, Beljaars ACM, van de Berg L, Bidlot J, Bormann N, Delsol C, Dragani R, Fuentes M, Geer AJ, Haimberger L, Healy SB, Hersbach H, Hólm EV, Isaksen L, Kallberg P, Kohler M, Matricardi M, McNally AP, Monge-Sanz BM, Morcrette JJ, Park BK, Peubey C, de Rosnay P, Tavolato C, Thépaut JN, Vitart F (2011) The ERA-Interim reanalysis: configuration and performance of the data assimilation system. *Q J R Meteorol Soc* 137:553–597
- Dimri AP (2004) Impact of horizontal model resolution and orography on the simulation of a western disturbance and its associated precipitation. *Meteorol Appl* 11:115–127
- Dimri AP, Mohanty UC, Azadi M, Rathore LS (2006) Numerical study of western disturbances over western Himalayas using mesoscale model. *Mausam* 57(4):579–590
- Dimri AP (2009) Impact of subgrid scale scheme on topography and landuse for better regional scale simulation of meteorological variables over the Western Himalayas. *Clim Dyn* 32:565–574
- Dimri AP (2012) Wintertime land surface characteristics in climatic simulations over the western Himalayas. *J Earth Syst Sci* 121(2):329–344
- Dimri AP, Chevuturi A (2014) Model sensitivity analysis study for western disturbances over the Himalayas. *Meteorol Atmos Phys* 123(3–4):155–180
- Dimri AP, Ganju A (2007) Wintertime seasonal scale simulation over Western Himalaya using RegCM3. *Pure Appl Geophys* 164(8–9):1733–1746
- Dimri AP, Mohanty UC (2009) Simulation of mesoscale features associated with intense western disturbances over western Himalayas. *Meteorol Appl* 16:289–308
- Dimri AP, Niyogi D (2012) Regional climate model application at subgrid scale on Indian winter monsoon over the western Himalayas. *Int J Climatol* 33(9):2185–2205
- Dimri AP, Mohanty UC, Mandal M (2004) Simulation of heavy precipitation associated with an intense western disturbance over western Himalayas. *Nat Hazards* 31:499–552
- Dimri AP, Yasunari T, Wiltshire A, Kumar P, Mathison C, Ridley J, Jacob D (2013) Application of regional climate models to the Indian winter monsoon over the western Himalayas. *Sci Total Environ* 468–469:S36–S47. <http://dx.doi.org/10.1016/j.scitotenv.2013.01.040>
- Gregory D, Rowntree PR (1990) A mass flux convection scheme with representation of cloud ensemble characteristics and stability dependent closure. *Mon Weather Rev* 118:1483–1506
- Gupta SC, Mandal GS (1987) Behaviour of kinetic energy generation function during a western disturbance in May 1982. *Mausam* 38(1):97–102
- Gupta A, Rathore LS, Singh SV, Mendiratta N (1999) Performance of a global circulation model in predicting the winter systems and associated precipitation over North West India during 1994–97. In: Dash SK, Bhadur J (eds) *The Himalayan environment*. New Age International Pvt. Ltd, New Delhi, pp 123–138
- Hara M, Kimura F, Yasunari T (2004) The generating mechanism of western disturbances over the Himalayas. In: 6th international GAME conference.
- Hatwar HR, Yadav BP, Rao YVR (2005) Prediction of western disturbances and associated weather over Western Himalayas. *Curr Sci* 88(6):913–920
- Heymsfield AJ, Miloshevich LM, Schmitt C, Bansemmer A, Twohy C, Poellot MR, Fridlind A, Gerber H (2005) Homogeneous ice nucleation in subtropical and tropical convection and its influence on cirrus anvil microphysics. *J Atmos Sci* 62:41–64
- Hoskins BJ, Karoly DJ (1982) The steady linear response of a spherical Atmosphere to thermal and Orographic forcings. *J Atmos Sci* 38:1179–1196
- Houghton JT (1987) Importance of satellites for weather forecasting. *Nature* 326:450–450. doi:10.1038/326450a0
- Houze RA Jr (2012) Orographic effects on precipitating clouds. *Rev Geophys* 50:1–47
- IMD (2013) A preliminary report on heavy rainfall over Uttarakhand during 16–18 June 2013. http://www.imd.gov.in/doc/uttarakhand_report_04_09_2013.pdf, Accessed on 20 Mar 2014

- Jacob D, Bäring L, Christensen OB, Christensen JH, de Castro M, Déqué M, Giorgi F, Hagemann S, Hirschi M, Jones R, Kjellström E, Lenderink G, Rockel B, Schär C, Seneviratne SI, Somot S, van Ulden A, van den Hurk B (2007) An inter-comparison of regional climate models for Europe: model performance in present day climate. *Clim Change* 81:31–52. doi:[10.1007/s10584-006-9213-4](https://doi.org/10.1007/s10584-006-9213-4)
- Kala CP (2014) Deluge, disaster and development in Uttarakhand Himalayan region of India: Challenges and lessons for disaster management. *Int J Disaster Risk Reduct* 8:143–152
- Kalsi SR, Halder SR (1992) Satellite observations of interaction between tropics and mid-latitudes. *Mausam* 43(1):59–64
- Krishnamurti TN, Kumar A, Yap KS, Dastoor AP, Davidson N, Sheng J (1990) Performance of a high resolution mesoscale tropical prediction model. *Adv Geophys* 32:133–286
- Lang TJ, Barros AP (2002) An Investigation of the Onsets of the 1999 and 2000 Monsoons in Central Nepal. *Mon Weather Rev* 130:1299–1316
- Lang TJ, Barros AP (2004) Winter storms in central Himalayas. *J Meteorol Soc Jap* 82(3):829–844
- Leung LR, Ghan SJ (1995) A subgrid parameterization of orographic precipitation. *Theor Appl Climatol* 52:95–118
- Lin Y-L, Chiao S, Wang T-A, Kaplan ML, Weglarz RP (2001) Some common ingredients for heavy orographic rainfall. *Weather Forecast* 16:633–660
- Liu X, Yanai M (2002) Influence of Eurasian spring snow cover on Asian summer rainfall. *Int J Climatol* 22:1075–1089
- Malurkar SL (1947) Abnormally dry and wet western disturbances over north India. *Curr Sci* 16(5):139–141
- Mohanty UC, Dimri AP (2004) Location-specific prediction of the probability of occurrence and quantity of precipitation over the Western Himalayas. *Weather Forecast* 19(3):520–533
- Mohanty UC, Madan OP, Rao PLS, Raju PVS (1998) Meteorological fields associated with western disturbances in relation to glacier basins of western Himalayas during winter season. Technical report, Centre for Atmospheric Science, IIT, Delhi, India
- Mohanty UC, Madan OP, Raju PVS, Bhatla R, Rao PLS (1999) A study on certain dynamic and thermodynamic aspects associated with western disturbances over north-west Himalaya. In: Dash SK, Bhadur J (eds) *The Himalayan environment*. New Age International Pvt. Ltd, New Delhi, pp 113–122
- Mull S, Desai BN (1947) The origin and structure of the winter depression of Northwest India. India Meteorological Department, Technical note No. 25:18
- Nigam S, Lindzen RS (1989) The sensitivity of stationary waves to variations in the basic state zonal flow. *J Atmos Sci* 46:1746–1768
- Pandey P, Pandey AK (2014) Uttarakhand disaster of June 2013: Geological issues of a Himalayan state. Personal Communication.
- Pisharoty P, Desai BN (1956) “Western disturbances” and Indian weather. *Indian J Meteorol Geophys* 7:333–338
- Puranik DM, Karekar RN (2009) Western disturbances seen with AMSU-B and infrared sensors. *J Earth Syst Sci* 118(1):27–39
- Raju PVS, Bhatla R, Mohanty UC (2011) A study on certain aspects of kinetic energy associated with western disturbances over northwest India. *Atmós* 24(4):375–384
- Rakesh V, Singh R, Yliya D, Pal PK, Joshi PC (2009) Impact of variational assimilation of MODIS thermodynamic profiles in the simulation of western disturbance. *Int J Remote Sens* 30(18):4867–4887
- Ramanathan Y, Saha KR (1972) Application of a primitive equation barotropic model to predict movement of “Western Disturbances”. *J Appl Meteorol* 11:268–272
- Ramasastri KS (1999) Snow melt modeling studies in India. In: Dash SK, Bahadur J (eds) *The Himalayan environment*. New Age International, New Delhi, pp 59–70
- Rao NSB, Moray PE (1971) Cloud systems associated with western disturbances: A preliminary study. *Indian J Meteorol Geophys* 22:413–420

- Rao VB, Rao ST (1971) A theoretical and synoptic study of western disturbances. *Pure Appl Geophys* 90(7):193–208
- Roe GH (2005) Orographic precipitation. *Annu Rev Earth Planet Sci* 33:645–671
- Roy SS, Bhowmik SKR (2005) Analysis of thermodynamics of the atmosphere over northwest India during the passage of a western disturbance as revealed by model analysis field. *Curr Sci* 88(6):947–951
- Schiemann R, Luthi D, Schar C (2009) Seasonality and interannual variability of the westerly jet in the Tibetan Plateau region. *J Clim* 22:2940–2957
- Semwal G, Dimri AP (2012) Impact of initial and boundary conditions on simulations of western disturbances and associated precipitation. *Nat Hazards* 64(2):1405–1424
- Semwal G, Giri RK (2007) Precipitation simulation of synoptic scale systems over western Himalayan region using Advanced Regional Prediction System (ARPS) model. *Mausam* 58(4):471–480
- Sharma RV, Subramaniam DV (1983) The western disturbance of 22 December 1980: A case study. *Mausam* 34(1):117–120
- Singh MS, Agnihotri CL (1977) Baroclinity over India in winter and its relation to western disturbances and jet streams – Part I. *Indian J Meteorol Hydrol Geophys* 28(3):303–310
- Smith RB (2006) Progress on the theory of orographic precipitation. *Spec Pap Geol Soc Am* 398:1–16
- Srinivasan V (1971) Some case studies of cirriform clouds over India during the winter period. *Indian J Meteorol Geophys* 22:421–428
- Srinivasan K, Ganju A, Sharma SS (2005) Usefulness of mesoscale weather forecast for avalanche forecasting. *Curr Sci* 88(6):921–926
- Tang H, Micheels A, Eronen JS, Ahrens B, Fortelius M (2013) Asynchronous responses of East Asian and Indian summer monsoons to mountain uplift shown by regional climate modeling experiments. *Clim Dyn* 40:1531–1549
- Thayyen RJ, Dimri AP, Kumar P, Agnihotri G (2012) Study of cloudburst and flash floods around Leh, India during August 4–6, 2010. *Nat Hazards* 65:2175–2204. doi:[10.1007/s11069-012-0464-2](https://doi.org/10.1007/s11069-012-0464-2)
- Thomas L, Dash SK, Mohanty UC (2013) Influence of various land surface parameterization schemes on the simulation of the western disturbances. *Meteorol Appl*. doi:[10.1002/met.1386](https://doi.org/10.1002/met.1386)
- Tiedtke M (1989) A comprehensive mass flux scheme for cumulus parameterization in large scale models. *Mon Weather Rev* 117:1779–1800
- Veeraraghavan K, Nath T (1989) A satellite study of an active western disturbance. *Mausam* 40(3):303–306
- Yadav RK, RupaKumar K, Rajeevan M (2012) Characteristic features of winter precipitation and its variability over northwest India. *J Earth Syst Sci* 121(3):611–623
- Yatagai A, Kamiguchi K, Arakawa O, Hamada A, Yasutomi N, Kitoh A (2012) APHRODITE: constructing a long term daily gridded precipitation dataset for Asia based on a dense network of rain Gauges. *Bull Am Meteorol Soc*. doi:[10.1175/BAMS-D-11-00122.1](https://doi.org/10.1175/BAMS-D-11-00122.1)